

# ACOUSTIC EMISSION INVESTIGATION OF LAMINATED TIMBER-CONCRETE TEST BEAMS

ISTVÁN SZŰCS<sup>1</sup>, JENO BALOGH<sup>2</sup> & ROSE HOLTZMAN<sup>2</sup>

<sup>1</sup>University of Pécs, Hungary.

<sup>2</sup>Metropolitan State University of Denver, USA.

## ABSTRACT

Laminated timber-concrete (LTC) and steel-timber-concrete composite beam (S-LTC) members with adhesive interlayer connections were experimentally investigated. This paper presents the results of the acoustic emission (AE) investigation performed during short-term static ramp-loading to failure tests. The beam specimens were continuously monitored using accelerometers connected to a four channel dynamic signal analyzer. For LTC beams, the failure of the timber in tension was typically observed; therefore, a steel layer was added to the tension side of the timber layer to increase the strength and to induce a ductile behaviour. The results of the AE investigations on two LTC and two S-LTC specimens reveal the progression of the failure as it initiates and gradually develops within the beams, leading to the tension failure and shear failure modes for the LTC and S-LTC specimens, respectively. The results confirm that the fast Fourier transformation (FFT) and waterfall type of spectral analysis have an important role in supplying substantial and reliable amounts of information for the identification of different phenomena in connection with the failure process of the investigated structural members.

**Keywords:** Acoustic emissions, Adhesive connection, Laminated structural members, Timber-concrete composite beams, Waterfall spectral analysis

## 1 INTRODUCTION

Timber-concrete composite structural members consist of a concrete layer placed on top of a timber layer with a shear connection. In this study, an adhesive-based inter-layer connection was used to create the laminated timber-concrete (LTC) members, providing for a continuous, high stiffness, simple constructible connection. These qualities were confirmed by several experimental investigations [1–7]. The typical observed primary failure mode was of the timber layer in tension. In a prior study [8], a carbon-fibre reinforced polymer (CFRP) layer was added to the tension fibres of the timber layer to prevent the tension failure, allowing for an increase in the load capacity. The failure-mode of the CFRP-LTC beams shifted to a shear failure on the full length of the timber layer. The secondary failure mode observed was typically the fracture of the concrete at the loading point. However, all these failure types are brittle and, it was found [8] that these could occur in a very short time sequence, making the experimental investigations of such members difficult when only strains, displacements, and loads are recorded. Consequently, acoustic emission (AE) monitoring was performed during the load testing of LTC specimens in order to build a more demonstrative picture about the investigated processes.

The investigative mind is mainly visual. In the rank of human senses hearing is put in second place because it often delivers less information to our perception system than vision. This might be the reason why audible acoustic phenomena during loading processes were regarded for a long time as a natural feature of the failure. Only in the past few decades, in line with the rapid development of measurement and computer techniques, was increasing attention paid to joint load tests and AE investigations of different structures in civil engineering [9–11].

A continuous AE activity monitoring of a short-term static ramp-loading to failure test may result in the processing of thousands of independent signals, even if only in the audible frequency range. Conventional techniques can be used to listen to AE events generated from

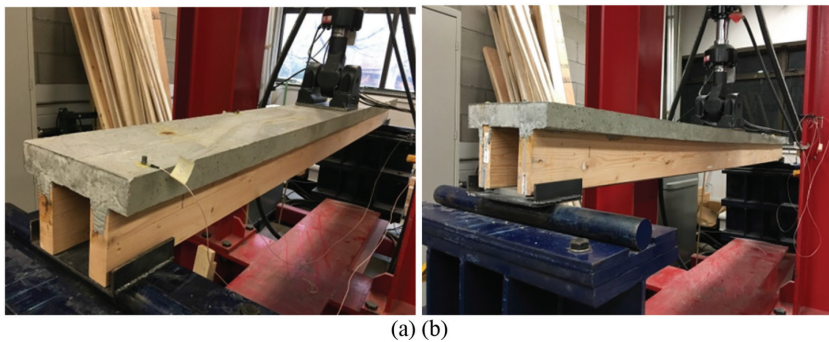


Figure 1: Typical beam specimens (a) LTC; (b) S-LTC.

the investigated material using sensors that function like the material scientist's stethoscope. Despite that the usual patterns of the waveform series of detected AE signals in the time domain produce a reliable amount of statistical information about the number and intensity of events in connection with the emitted energy releases, a completion of our data processing arsenal with a frequency – time domain visualization may promote a more sophisticated interpretation.

An advanced frequency – time domain waterfall type spectrogram analysis proved to be a promising supplementary tool to visualize and distinguish some of the failure mechanisms of composite beams.

This paper presents the results of the AE investigations performed on four LTC beam specimens at Metropolitan State University of Denver (MSU Denver). Two of the beams were regular LTC beams (Fig. 1a), while the other two were steel-reinforced LTC members (Fig. 1b). Steel was embedded into the timber layer, replacing the CFRP used in a prior study [8] in order to confer ductility to the specimen behaviour.

## 2 MEASUREMENT AND DATA PROCESSING SYSTEM

AE testing was performed with a Brüel/Kjaer PHOTON+™ dynamic signal analysis system, converting a notebook computer into an instrument-quality multi-channel analyzer with 115 dB dynamic range and with a 84.2 kHz real-time rate. This data collection system was equipped with four B/K 4397 accelerometers with resonance frequencies between 45.7 and 55.7 kHz, that were installed in the same configuration, see Figure 2, on all of the laminated

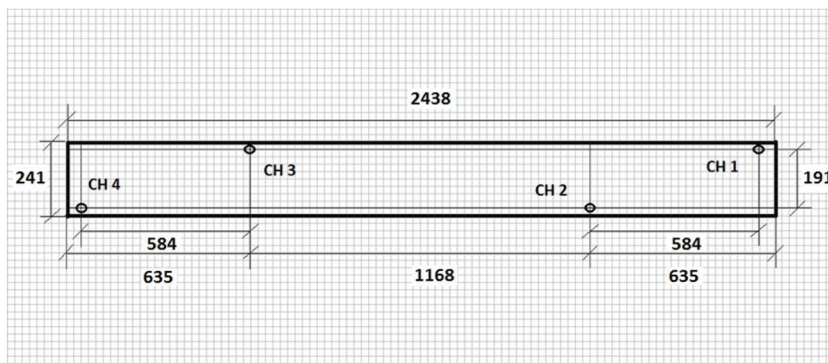


Figure 2: Layout of the accelerometers on the beams [mm].

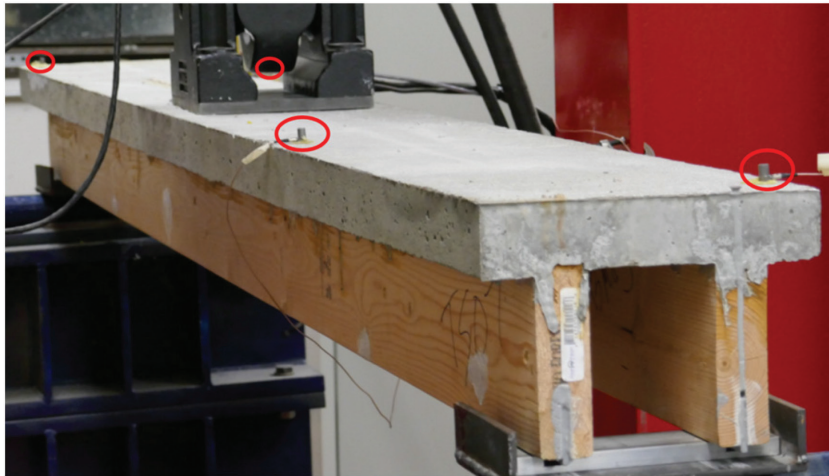


Figure 3: Accelerometers attached to an S-LTC specimen.

beams specimens. The mounting of the four accelerometers on an S-LTC beam in the loading frame is shown on Figure 3.

For mechanical coupling of the sensors to the beams, a mounting wax was used. A teflon insulated double-screened cable (type AO1381) connected all of the accelerometers with built-in preamplifiers to the data acquisition system.

Voltage ranges from 10 mV to 10 V were provided by programmable gain stages on the inputs. Analog and digital filters on all inputs guaranteed a complete alias protection ensuring full data integrity. This design, together with the 24-bit resolution, resulted in an extremely low noise floor; a requirement for acoustic measurements; and high accuracy. The quick measurement setup, combined with real time indication of the detected signals, by means of RT Pro™ 7.2 software available at MSU Denver, enabled a continuous monitoring validation, recording and post-processing of the data both in the time and frequency range, see Figure 4.

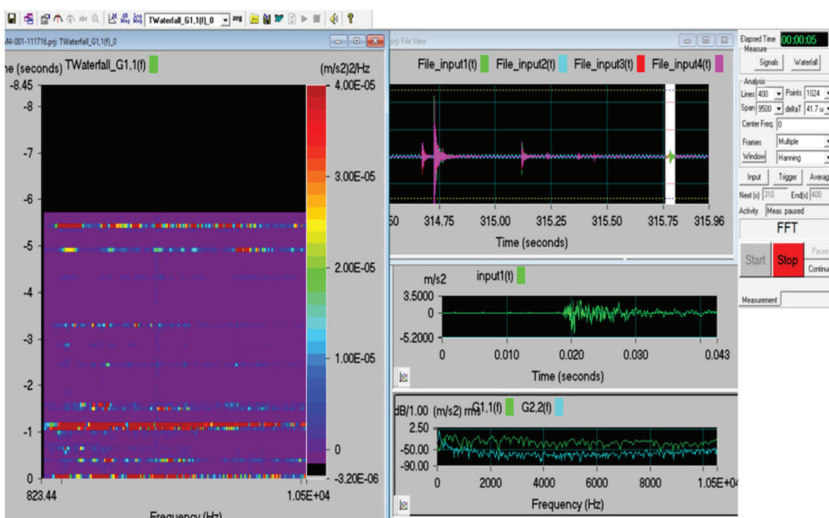


Figure 4: A real time monitoring screenshot of AE signals in time and frequency domain.

### 3 DATA PROCESSING AND EVALUATION

Conventional techniques can be used for time domain data acquisition and evaluation of AE events generated in the structural member investigated, which contain thousands of independent signals to be processed, even if only in the audible frequency range. While the wavelet series of detected AE signals in the time domain produce a reliable amount of statistical information about the number and intensity of events, a frequency – time domain visualization may facilitate an advanced interpretation on the basis of spectrogram analysis.

#### 3.1 Fundamentals

The four-channel monitoring of the complete load test process ranging from 400 to 700 seconds produced a considerably higher amount of AE signals in the final stage of the observation approaching the failure. Thus the evaluation focused on the last 100 seconds of the records, specifically on the distribution of the number and intensity of AE signals generated in the four beams (BM1, BM3, BM4 and BM5) investigated and on the mutual correlations of these parameters, including load levels applied.

##### 3.1.1 AE number and intensity

The main significant features of the detected AE signals (number of AE signals/channels, AE (peak) intensity, average intensity/AE) derived from the last 100 seconds of the loading period recorded for four beams are summarized in Table 1. BM1 and BM3 are LTC-, while BM4 and BM5 are S-LTC beams. The AE intensity was defined as the peak values of each independent burst type transients. The continuous type acoustic emissions in the observed frequency range were disregarded, not because of the negligible number but because of the very low levels and signal/noise ratio of them.

For the final loading stages approaching the failure of the beams BM1, BM3–BM5 the traces of the load levels and acoustic parameters are presented together on Figures 5–8, respectively.

##### 3.1.2 Correlations

The most significant correlations are displayed in Figures 5–8 showing visual evidence of the strong relations between the main load drops and main AE intensity peaks with the exception of the time interval between 360–365 seconds of BM1 load test, representing the lack of AE intensity during load drop in Figure 5. This discrepancy can be interpreted as a presence of a substantial material anomaly or – explained with the Kaiser effect – it may indicate a former higher load impact which exceeded the actual one. Likewise, the behaviour of BM3 shown in Figure 6: it emits notable AE intensity only after the primary load level is exceeded at 443 seconds. Nevertheless, before this moment, at a load below the previous maximum, a large amount of very low level signal was emitted with insignificant AE intensity in accordance with the Felicity effect.

Table 1: Main calculated parameters of the detected AE signals.

Number of AE signals/Ch.		AE (peak) Intensity [m/s <sup>2</sup> ]		Average Int/AE [m/s <sup>2</sup> ]
Total	Average/s	Total	Average/s	
BM1	30	0.65	229.44	4.98
BM3	388	3.76	789.96	7.76
BM4	132	1.52	848.35	9.75
BM5	160	1.48	530.29	4.91

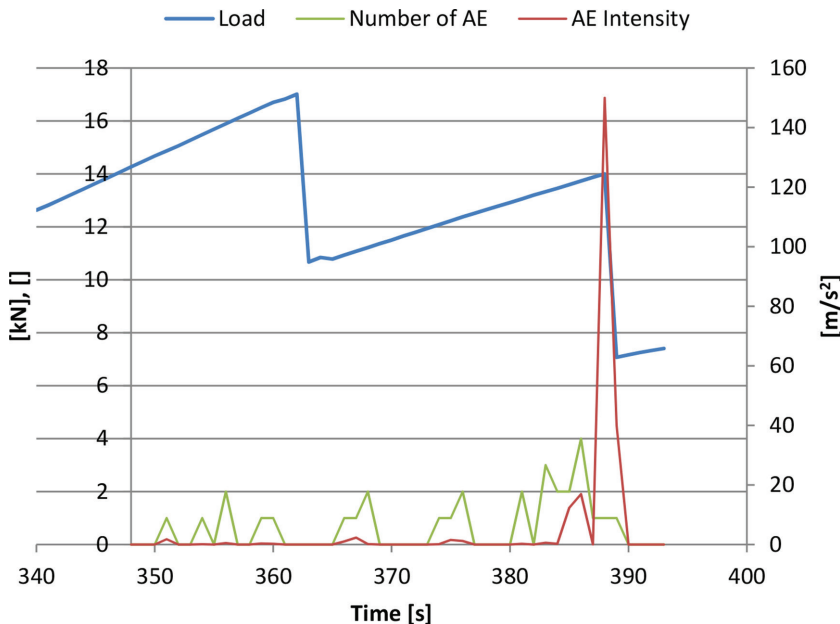


Figure 5: Load levels and AE parameters for BM1.

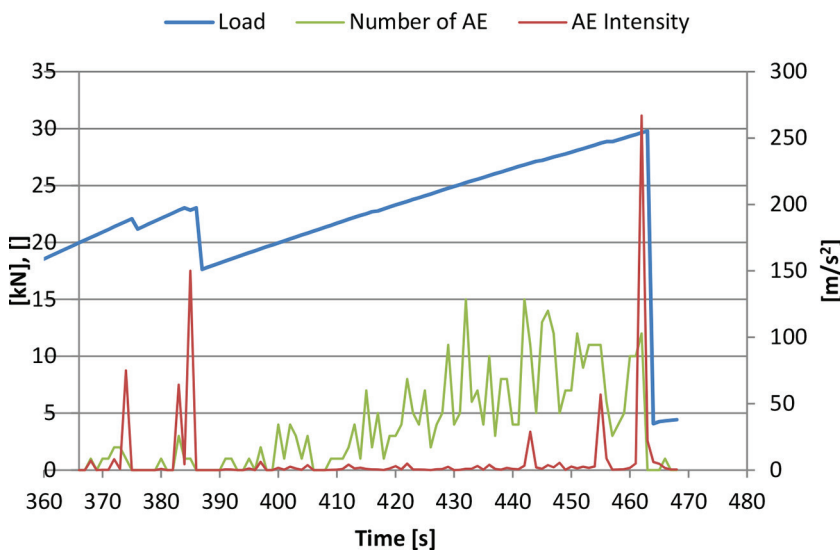


Figure 6: Load levels and AE parameters for BM3.

The visual correlation between AE intensity and number is much less significant. The higher values calculated and summarized in Table 2 are restricted to the short time domain (-5s) represented by stable increasing rates preceding the impending final failure. However, the correlation coefficients between AE intensities are higher than 0.96 for any combination of different beams behaviour in the final 10 seconds.

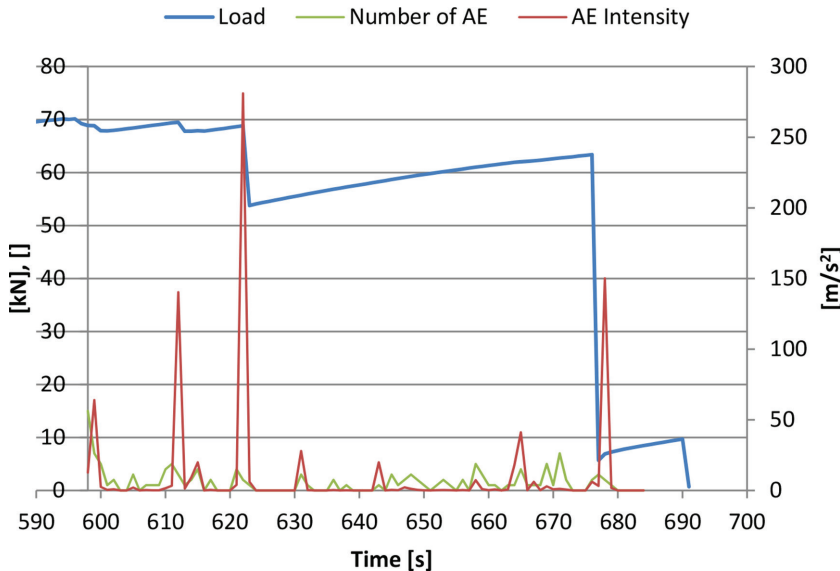


Figure 7: Load levels and AE parameters for BM4.

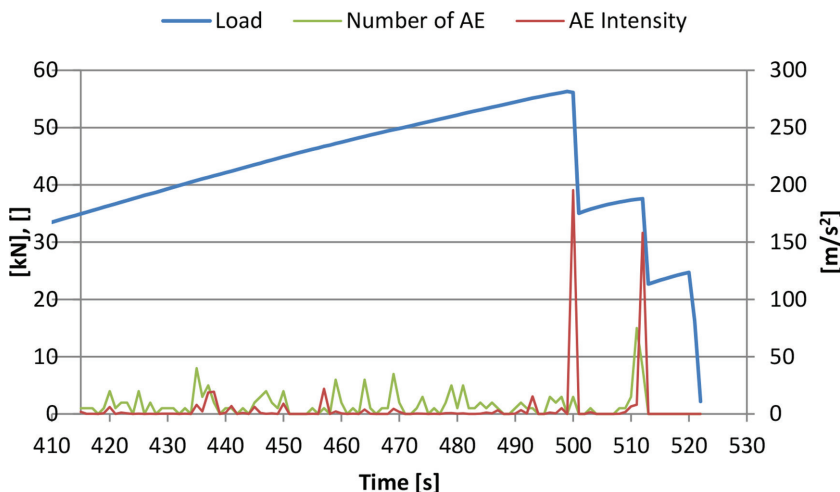


Figure 8: Load levels and AE parameters for BM5.

Table 2: Correlation coefficient between AE intensity and number.

Time domain before final failure [s]	Correlation coefficient between AE intensity and number			
	BM1	BM3	BM4	BM5
-5	0.82	0.77	0.77	0.79
-10	0.66	0.37	0.34	0.85
-15	0.64	0.30	0.25	0.12

### 3.2 Spectrogram analysis

Spectrograms are usually created in one of two ways:

- approximated as a filterbank that results from a series of bandpass filters:

$$G(\omega, t) = \int_0^{\omega} F(\phi) h(\omega - \phi) e^{-j\phi t} d\phi \quad (1)$$

- calculated from the  $f(\tau)$  time signal using the fast Fourier transformation (FFT):

$$G(\omega, t) = \int_0^t f(\tau) g(t - \tau) e^{-j\omega t} d\tau \quad (2)$$

The bandpass filters method (1) typically uses analog processing to divide the input signal into frequency bands.

Creating a spectrogram using the FFT (2) on the other hand is a digital process. The sampled data, in the time domain, is broken up into segments, which usually overlap, and Fourier transformed to calculate magnitude – frequency spectrum for each segment. The series of spectra are laid side by side to form an image like a three-dimensional surface.

Figure 9 shows the acceleration – time function (left) and the relating FFT spectrogram (right, produced by means of RT Pro™ 7.2 software) of the AE activity in BM4 during the last 100 seconds of loading test. The main transients in time domain (left) and the corresponding horizontal slices of frequency spectra (right) can be easily identified.

### 3.3 Evaluation of rupture sizes

The FFT spectrograms displaying large amount of compacted information are very useful tools in the efficient evaluation of load test history. During the investigation of the BM1

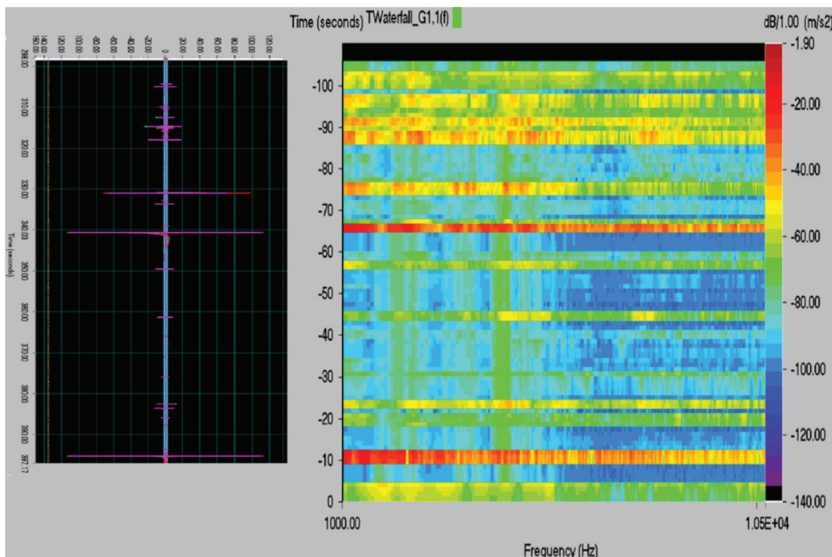


Figure 9: Time function (left) and a FFT spectrogram (right) of the AE activity in BM4.

– BM5 beams we have recorded thousands of AE signals in the measured frequency range. In the analysis, focus was given to the AE signals, whose numbers (altogether 710 transients, multiplied by four channels) are indicated in the left column of Table 1. The vast compressive capacity of spectrogram analysis proved to be a productive instrument in finding new conclusions. Figure 10 (top) illustrates a short time (2 seconds) wavelet train (containing six transient signals indicated with 1–6) from the AE database of BM3 (in the interval of the loading phase encircled in red in Figure 10, right bottom). The corresponding spectrogram (Fig. 10, left bottom) presents not only their sequential appearance in time but inform us about the frequency contents of each signal.

For example, we can directly analyze the corner frequencies of the succeeding individual AE signals, each of them represent an emitted energy release originating from a given source size ( $R$ ) which is inversely proportional to the corner frequency ( $f$ ) and directly to the wave propagation velocity. The positioning of accelerometers, shown in Figure 2 and Figure 3, allows for the use of the following formula, based on Hardy [12], containing the share wave velocity ( $v_s$ ) value:  $R = 2.34 \times v_s / 2\pi f$ . The estimated source size growth range (a doubling, due to the corner frequency drop from 10 kHz to 5 kHz) is between 8 and 16 cm. This is coincidental with the time domain, characterized by large amounts of very low level signals emitted with insignificant AE intensity (described in 3.1.2) indicating an enlargement of an already existing failure generated during the previous load level maximum.

### 3.4 Failure mechanism pattern types

In connection with the developing failure mechanism in the investigated laminated beam structures reflected by the AE spectrogram patterns studied, the following four different types could be identified:

- forerunning AE series, decreasing corner frequencies, no/small closing failure (Fig. 11, top left);

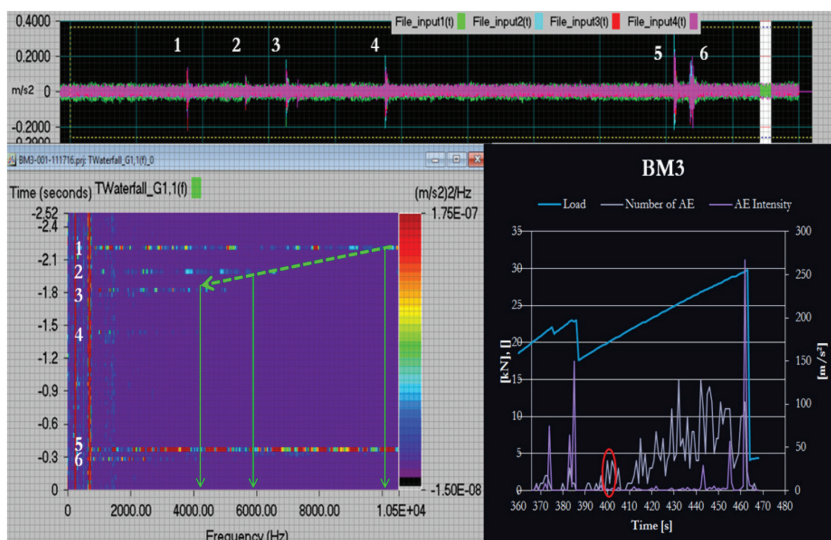


Figure 10: Evaluation of rupture sizes by means of corner frequencies in BM3.

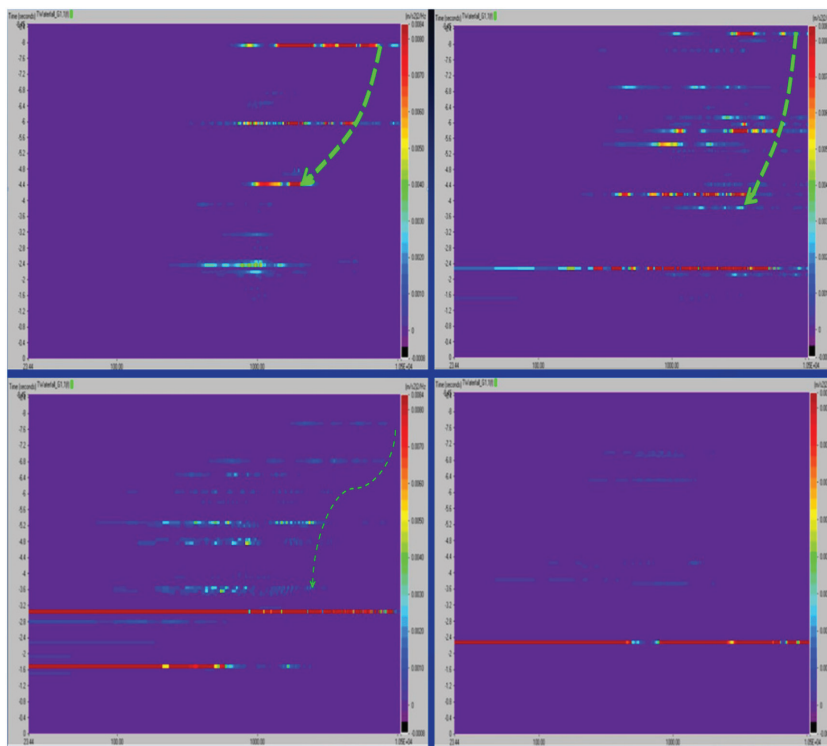


Figure 11: Identified types of developing failure mechanisms.

- forerunning AE series, decreasing corner frequencies, substantial closing failure (Fig. 11, top right);
- decreased forerunning AE series, decreasing corner frequencies, closing failure (Fig. 11, bottom left);
- almost full lack of forerunning AE series, closing failure (Fig. 11, bottom right).

The indicative corner frequencies and their trends are highlighted with green dashed lines.

#### 4 CONCLUSIONS

AE test investigations performed on 4-channel Brüel/Kjaer PHOTON+™ System equipped with 4397 type accelerometers proved to be an adequate tool for continuous monitoring of LTC and S-LTC beam load test process both in time and spectral domain. The results demonstrate a wide range of data processing segments and confirm that the applied FFT and waterfall type spectral analysis may have an important and pioneering role in concentrating and supplying reliable amount of substantial information for:

- imaging, visualizing and evaluating a load test process of different laminated beam structures to be applied in civil engineering constructions;
- identification of different spectral patterns phenomena in connection with the failure mechanism of the investigated structures.

### ACKNOWLEDGEMENTS

The research was performed within the framework of the institutional cooperation between University of Pecs and MSU Denver. The present scientific contribution is dedicated to the 650th anniversary of the foundation of the University of Pécs, Hungary. The authors are grateful to the MSU Denver students who assisted with the laboratory specimen construction and experimental setup.

### REFERENCES

- [1] Balogh, J., Laminated wood-concrete structural members. *Pollack Periodica, An International Journal for Engineering and Information Sciences*, **8**(3), pp. 79–86, 2013. <https://doi.org/10.1556/pollack.8.2013.3.8>
- [2] Shrestha, R., Mark, J. & Crews, K., Experimental investigation on epoxy bonded shear connection for timber-concrete composites. *Proceedings of the World Conference on Timber Engineering (WCTE 2012)*, **3**, pp. 466–472, 2012.
- [3] Henrique, J., Oliveira, J.D., Miguel, F., Oliveira M.D., Alexandra, C., Oliveira, L.D. & Cachim, P.B., Glued composite timber-concrete beams. I: Interlayer connection specimen tests. *Journal of Structural Engineering, ASCE*, **136**(10), pp. 1236–1245, 2010. [https://doi.org/10.1061/\(asce\)st.1943-541x.0000228](https://doi.org/10.1061/(asce)st.1943-541x.0000228)
- [4] Henrique, J., Oliveira, J.D., Miguel, F., Oliveira M.D., Alexandra, C., Oliveira, L.D. & Cachim, P.B., Glued composite timber-concrete beams. II: Analysis and tests of beam specimens. *Journal of Structural Engineering, ASCE*, **136**(10), pp. 1245–1254, 2010. [https://doi.org/10.1061/\(asce\)st.1943-541x.0000251](https://doi.org/10.1061/(asce)st.1943-541x.0000251)
- [5] Brunner, M., Romer, M. & Schnuriger, M., Timber-concrete-composite with an adhesive connector. *Materials and Structures*, **40**, pp. 15–25, 2006.
- [6] Clouston, P., Bathon, L.A. & Schreyer, A., Shear and bending performance of a novel wood-concrete composite system, *Journal of Structural Engineering, ASCE*, **131**(9), pp. 1404–1412, 2005. [https://doi.org/10.1061/\(asce\)0733-9445\(2005\)131:9\(1404\)](https://doi.org/10.1061/(asce)0733-9445(2005)131:9(1404))
- [7] Gutkowski, R.M., Balogh, J. & To, L.G., Finite-element modeling of short-term field response of composite wood-concrete floors/decks. *Journal of Structural Engineering, ASCE*, **136**(6), pp. 707–714, 2010. [https://doi.org/10.1061/\(asce\)st.1943-541x.0000117](https://doi.org/10.1061/(asce)st.1943-541x.0000117)
- [8] Balogh, J., High performance CFRP-timber-concrete laminated composite members. *Proceedings of the World Conference on Timber Engineering (WCTE 2016)*, 2016.
- [9] Varner, D., Acoustic emission during static bending of wood specimens. *Dissertation, Mendel University in Brno*, 2012.
- [10] Kaphle, M.R., Analysis of acoustic emission data for accurate damage assessment for structural health monitoring applications. *PhD thesis, Queensland University of Technology*, 2012.
- [11] Szucs, I. & Deak, F., Examination of a granitic host rock behaviour around underground radwaste repository chambers based on acoustic emission datasets, *Rock Mechanics and Rock Engineering: From the Past to the Future – Ulusay et al. (Eds.) Taylor & Francis Group, London*, 2016.
- [12] Hardy, R., Acoustic emission/ microseismic activity. *Pennsylvania State University, Taylor and Francis e-Library*, pp. 244, 2005.